

TABLE I. Ionization potentials for Al, Al<sub>2</sub>, and their oxides, from Refs. 9 and 10.

	Al	Al <sub>2</sub>
Al <sub>n</sub>	5.99	~ 6.0
Al <sub>n</sub> O	9.5	~ 8.0
Al <sub>n</sub> O <sub>2</sub>	...	~10.0

What is responsible for the observed product distributions? Thermodynamics probably plays an important role. Table I shows ionization potentials for Al, Al<sub>2</sub>, and their oxides.<sup>9,10</sup> Adding oxygen to Al and Al<sub>2</sub> raises their ionization potentials. If this occurs for the larger clusters it provides an explanation for why oxide product ions are not observed: The charge goes to the product with the lower ionization potential. There are subtle indications in the product distributions that Al<sub>7</sub><sup>+</sup> and Al<sub>14</sub><sup>+</sup> (the magic numbers) are slightly favored products. Loss of Al<sub>10</sub> is observed first for Al<sub>17</sub><sup>+</sup> yielding Al<sub>7</sub><sup>+</sup>, and the switch from Al<sub>4</sub> to Al<sub>5</sub> loss for Al<sub>19</sub><sup>+</sup> results in production of Al<sub>14</sub><sup>+</sup>. If thermodynamics plays a major role in determining the products, then our results indicate that (Al<sub>4</sub>O<sub>2</sub>), (Al<sub>5</sub>O<sub>2</sub>), and (Al<sub>10</sub>O<sub>2</sub>) must be particularly stable. Unfortunately we do not know if (Al<sub>5</sub>O<sub>2</sub>) is Al<sub>5</sub>O<sub>2</sub>, for example it could be Al<sub>3</sub>O + Al<sub>2</sub>O; similarly (Al<sub>4</sub>O<sub>2</sub>) could be Al<sub>2</sub>O + Al<sub>2</sub>O. Al<sub>2</sub>O<sup>+</sup> and

Al<sub>3</sub>O<sup>+</sup> occur as intense ions in the mass spectrum from the source (see Fig. 1).

- <sup>1</sup>S. J. Riley, E. K. Parks, G. C. Nieman, L. G. Pobo, and S. Wexler, *J. Chem. Phys.* **80**, 1360 (1984); S. C. Richtmeier, R. K. Parks, K. Liu, L. G. Pobo, and S. J. Riley, *ibid.* **82**, 3659 (1985).  
<sup>2</sup>M. E. Geusic, M. D. Morse, and R. E. Smalley, *J. Chem. Phys.* **82**, 590 (1985); M. D. Morse, M. E. Geusic, J. R. Heath, and R. E. Smalley, **83**, 2293 (1985).  
<sup>3</sup>D. J. Trevor, R. L. Whetten, D. M. Cox, and A. Kaldor, *J. Am. Chem. Soc.* **107**, 518 (1985); R. L. Whetten, D. M. Cox, D. J. Trevor, and A. Kaldor, *J. Phys. Chem.* **89**, 566 (1985).  
<sup>4</sup>M. L. Mandich, W. D. Reents, and V. E. Bondybeay, *J. Phys. Chem.* **90**, 2281 (1986).  
<sup>5</sup>S. W. McElvany, W. R. Creasy, and A. O'Keefe, *J. Chem. Phys.* **85**, 632 (1986).  
<sup>6</sup>B. S. Larsen, R. B. Freas, and D. P. Ridge, *J. Phys. Chem.* **88**, 6014 (1984); D. B. Jacobson and B. S. Freiser, *J. Am. Chem. Soc.* **106**, 4623, 5351 (1984); K. Ervin, S. K. Loh, N. Aristov, and P. B. Armentrout, *J. Phys. Chem.* **87**, 3593 (1983); L. Hanley and S. L. Anderson, *Chem. Phys. Lett.* **122**, 410 (1985).  
<sup>7</sup>L. Wöste, presented at the International Symposium on Metal Clusters, Heidelberg, April, 1986.  
<sup>8</sup>D. M. Cox, D. J. Trevor, R. L. Whetten, E. A. Rohlfing, and A. Kaldor, *J. Chem. Phys.* **84**, 4651 (1986); M. E. Geusic and R. R. Freeman (private communication).  
<sup>9</sup>T. H. Upton, *Phys. Rev. Lett.* **56**, 2168 (1986).  
<sup>10</sup>H. M. Rosenstock, K. Draxl, B. W. Steiner, and J. T. Herron, *J. Phys. Chem. Ref. Data* **6**, Suppl. No. 1 (1977).

## Two-dimensional Fourier transform ESR spectroscopy<sup>a)</sup>

Jeff Gorcester and Jack H. Freed

*Baker Laboratory of Chemistry, Cornell University, Ithaca, New York 14853*

(Received 2 June 1986; accepted 27 August 1986)

The possibility of performing Fourier transform (FT)-ESR has very recently been demonstrated.<sup>1,2</sup> An important objective would be to perform a variety of 2D experiments<sup>3,4</sup> in much shorter time and to perform other 2D experiments only possible by FT methods.<sup>5</sup>

In this work we demonstrate the feasibility of such experiments with two examples in which an entire (fast motional) nitroxide ESR spectrum (total width of 90 MHz) is irradiated.

Our FT-ESR spectrometer is modified in several important respects from the electron-spin-echo (ESE) spectrometer<sup>6</sup> we previously utilized<sup>1,3,4</sup>: (1) a quadrature detector simultaneously yields the real and imaginary parts of the time-domain signal; (2) signal averaging is accomplished using a two-channel transient digitizer (HP54100A 1 GHz

oscilloscope); (3) high fidelity microwave pulses (50 ps jitter) are obtained from a modified<sup>7</sup> TWT amplifier.

The first example involves digitizing the echo after a  $\pi/2 - t_1 - \pi/2 - t_1 + t_2$  sequence. The procedure is repeated for a series of equally spaced values of  $t_1$ , and is then 2D Fourier transformed. The 2D-ESE spectrum (Fig. 1) is obtained after making a small first-order phase correction in  $\omega_2$  and a linear amplitude correction.<sup>1</sup> One observes the inhomogeneously broadened three-line hf pattern along  $\omega_2$  and the Lorentzian homogeneous line shapes along  $\omega_1$ . (A magnetic field gradient was introduced to suppress the FID from the second  $\pi/2$  pulse. This would not be necessary for a slow-motional spectrum.<sup>3,4</sup>) Note that the irradiation frequency  $\omega$ , is just below the low-frequency hf line yet the whole 90 MHz spectrum is successfully irradiated. This ex-

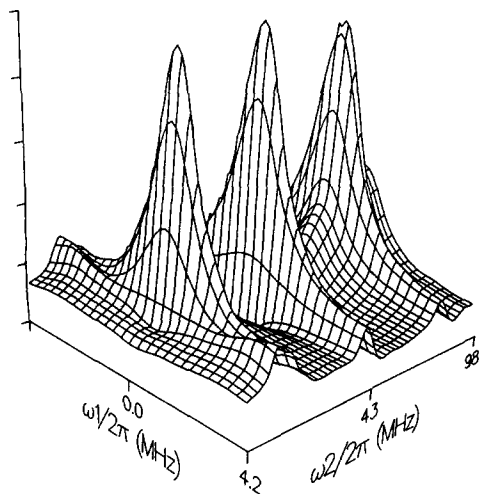


FIG. 1. 2D-ESE spectrum of  $\sim 2$  mM PD-tempone in toluene- $d_8$  at 22 °C by FT methods.  $T_1^* \approx 75$  ns;  $T_2 = 135$  ns; 0.86 ns resolution of echo providing 256 complex data points, each the average of 2048 transients. Time resolution in  $t_1$  is 6 ns, pulse width is 15 ns.

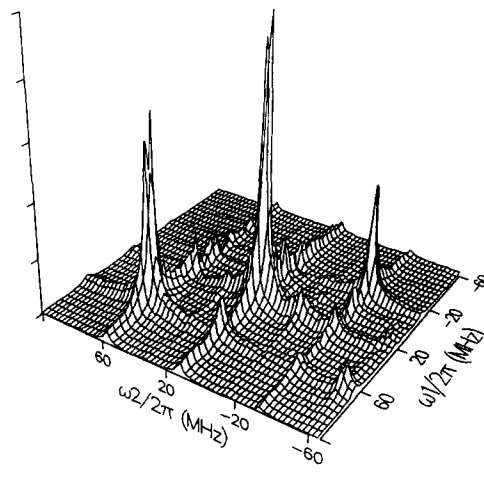


FIG. 2. 2D exchange spectrum of  $\sim 2$  mM PD-tempone in toluene- $d_8$  at 22 °C by FT methods.  $T_1^* \approx T_2 = 135$  ns; 3.3 ns resolution of FID providing 256 complex data points, each the average of 512 transients and requiring 8.6 s per FID. There are 70 values of  $t_1$  with 3 ns resolution. Dead time is 65 ns, pulse width is 16 ns, and  $T = 310$  ns.

ample is the FT-2D analog of the field-swept 2D experiment described in Ref. 3, and it reduces the time of the experiment by an order of magnitude. (We anticipate an additional order of magnitude reduction with modified equipment). Minor modifications to our current spectrometer design should make this technique the method of choice for 2D-ESE.<sup>3,8</sup>

The second example is from the category of 2D spin-exchange spectroscopies and is based upon the  $\pi/2 - t_1 - \pi/2 - T - \pi/2 - t_2$  Jeener-Ernst sequence.<sup>5</sup> This involves four time periods: preparation, evolution, mixing, and detection. The preparation period consists of a  $\pi/2$  pulse to generate the initial transverse magnetization. "Frequency labeling" occurs during the evolution period of duration  $t_1$ . The second  $\pi/2$  pulse starts the mixing period wherein the longitudinal magnetization components associated with each hf line can be exchanged, thereby mixing components carrying different precessional frequency information. Thus, after rotating this magnetization into the  $xy$  plane for detection, components initially precessing with angular frequency  $\omega_1 = \omega_a$  will, via magnetization transfer (MT), precess with new frequency  $\omega_2 = \omega_b$ . In our example, shown in Fig. 2, we rely on the significant Heisenberg-spin exchange (HE)<sup>9-11</sup> to produce the MT between the hf lines.<sup>12</sup>

This sequence is repeated for a series of equally spaced values of  $t_1$ . For each  $t_1$  the FID is collected, then the phase of the preparation pulse is advanced by 90°, and a second FID is collected [call them  $S'(t_1, t_2)$  and  $S''(t_1, t_2)$ ]. These two signals depend on terms oscillatory in  $t_1$  that are in phase quadrature.<sup>13</sup> FT of each data set yields  $|S'(t_1, \omega_2)|$  and  $|S''(t_1, \omega_2)|$ . Base line corrections facilitate removal of axial peaks,<sup>14</sup> after which we form

$$S(t_1, \omega_2) = |S'(t_1, \omega_2)| + i|S''(t_1, \omega_2)|,$$

which yields the desired 2D spectrum  $|S(\omega_1, \omega_2)|$  upon final FT.

This phase alternation scheme yields the required frequency discrimination in  $\omega_1$ , and it provides the phase information necessary for the pure absorption representation.<sup>15,16</sup> This should be useful for probes undergoing slow-tumbling motion for which the spectra are composed of very many "dynamic spin packets" DSP.<sup>3,4,12</sup> For such systems the 2D spectrum would lead to direct correlation of the MT<sup>4,12</sup> between DSP from different molecular orientations. This method may be regarded as a 2D analog of ELDOR.<sup>17-19</sup>

In our fast-motional example in Fig. 2, the diagonal peaks correspond to the three  $^{14}\text{N}$  hf lines, while the (six) off-diagonal peaks (where the values of  $\omega_1$  and  $\omega_2$  correspond to different hf frequencies) represent MT from one line to the other in accordance with the theory<sup>12,18</sup> applicable for the present case of the HE of the order of electron-spin relaxation.<sup>11,20</sup> In theory, the exchange rate constant,  $k_{\text{HE}}$  can be obtained by comparing the amplitudes of off-diagonal vs diagonal peaks (after correcting for known artifacts), but it is well-known<sup>21</sup> that this would permit only rough estimates. We found, in this manner, a value of  $k_{\text{HE}}$  about 28% ( $\pm 5\%$  from the different peaks) of the value  $3.1 \times 10^{-9} \text{ M}^{-1} \text{ s}^{-1}$  reported in Ref. 11. We expect substantially greater accuracy by varying<sup>4</sup>  $T$  in a series of such 2D experiments. (Spurious peaks, which do not come at the MT-peak positions, are due to imperfections in the quadrature detector. Also, there is a small contribution, only to the diagonal peaks, from the FID caused by the first pulse which freely precesses for the rest of the sequence. It could be eliminated by pulsed field-gradient techniques,<sup>5,19</sup> or by phase alteration schemes.<sup>21</sup>) Further improvements of this MT technique, as well as its variations,<sup>4</sup> should be of considerable value in studies of molecular dynamics.

<sup>a)</sup> Supported by NSF Grant No. CHE83-19826 and by NIH Grant No. GM25862.

<sup>1)</sup> J. P. Hornak and J. H. Freed, *J. Magn. Reson.* **67**, 501 (1986).

<sup>2)</sup> M. Bowman, *Bull. Am. Phys. Soc.* **31**, 524 (1986).

- <sup>3</sup>G. L. Millhauser and J. H. Freed, *J. Chem. Phys.* **81**, 37 (1984).  
<sup>4</sup>L. J. Schwartz, G. L. Millhauser, and J. H. Freed, *Chem. Phys. Lett.* **127**, 60 (1986).  
<sup>5</sup>J. Jeener, B. H. Meier, P. Bachmann, and R. R. Ernst, *J. Chem. Phys.* **71**, 11 (1979).  
<sup>6</sup>A. E. Stillman and R. N. Schwartz, *J. Phys. Chem.* **85**, 3031 (1981).  
<sup>7</sup>H. Borsboom (private communication).  
<sup>8</sup>R. P. J. Merks and R. deBeer, *J. Phys. Chem.* **83**, 3319 (1979).  
<sup>9</sup>J. H. Freed, *J. Chem. Phys.* **45**, 3452 (1966).  
<sup>10</sup>M. P. Eastman, R. G. Kooser, M. R. Das, and J. H. Freed, *J. Chem. Phys.* **51**, 2690 (1969).  
<sup>11</sup>R. N. Schwartz, L. L. Jones, and M. K. Bowman, *J. Phys. Chem.* **83**, 3429 (1979).  
<sup>12</sup>L. J. Schwartz, Ph.D. thesis Cornell University, 1984; L. J. Schwartz and J. H. Freed (to be published).  
<sup>13</sup>J. Keeler and D. Neuhaus, *J. Magn. Reson.* **63**, 454 (1985).  
<sup>14</sup>W. P. Aue, E. Bartholdi, and R. R. Ernst, *J. Chem. Phys.* **64**, 2229 (1976).  
<sup>15</sup>D. J. States, R. A. Haberkorn, and D. J. Ruben, *J. Magn. Reson.* **48**, 286 (1982).  
<sup>16</sup>P. Bachmann, W. P. Aue, L. Muller, and R. R. Ernst, *J. Magn. Reson.* **28**, 29 (1977).  
<sup>17</sup>J. S. Hyde, J. C. W. Chien, and Jack H. Freed, *J. Chem. Phys.* **48**, 4211 (1968).  
<sup>18</sup>J. H. Freed, in *Time Domain Electron Spin Resonance*, edited by L. N. Kevan and R. N. Schwartz (Wiley, New York, 1979), Chap. 2.  
<sup>19</sup>J. P. Hornak and J. H. Freed, *Chem. Phys. Lett.* **101**, 115 (1983).  
<sup>20</sup>J. S. Hwang, R. P. Mason, L. P. Hwang, and J. H. Freed, *J. Phys. Chem.* **79**, 489 (1975).  
<sup>21</sup>A. Bax, *Two-Dimensional Nuclear Magnetic Resonance in Liquids* (Reidel, Boston, 1984), pp. 95, 181, 61.

## NOTES

## Molecular beam studies of open-shell systems: The van der Waals interaction between O(<sup>3</sup>P) and He(<sup>1</sup>S)

V. Aquilanti, R. Candori, E. Luzzatti,<sup>a)</sup> F. Pirani, and G. G. Volpi  
*Dipartimento di Chimica dell'Università, 06100 Perugia, Italy*

(Received 2 June 1986; accepted 14 July 1986)

A first attempt to obtain information on the interaction between helium and ground state oxygen atoms was reported many years ago from this laboratory<sup>1</sup>: Only an estimate of the average potential could be given. Recently, an extensive computational study<sup>2</sup> has been devoted to this system, which is basic to our understanding of the nature of the interactions of open shell atoms. In this Note, new experimental results on this system are reported, and the available information is shown to provide an assessment of the main features of the involved interaction.

The results, which supersede the old ones, are shown in Fig. 1: The absolute integral cross sections have been obtained as a function of velocity employing the apparatus described previously<sup>3</sup> and used recently for the study of the interaction of F(<sup>2</sup>P) atoms with rare gases,<sup>4</sup> of O(<sup>3</sup>P) with Ar, Kr, and Xe,<sup>3</sup> of N atoms with Ar<sup>5</sup> and Kr.<sup>6</sup> The oxygen atom beam is velocity selected to better than 5%, and a Stern–Gerlach magnet (Rabi configuration) provides a control of the atomic magnetic sublevels.

These low energy integral cross section experiments can be interpreted by assuming that the collision takes place adiabatically along six effective potential energy curves, labeled by the quantum numbers of atomic angular momentum  $j = 2, 1, 0$  and its projection  $\Omega = |m_j|$ . These curves are related to the electrostatic potentials  $v_\Sigma$  and  $v_\Pi$  by the formulas given in the Appendix of Ref. 3.

A variation of the magnetic field intensity allows a variation of the relative population of the  $|j\Omega\rangle$  states: The results in Fig. 1 show that the difference of cross sections for

two extreme cases is minor, indicating that the anisotropy of the involved interaction is small.

A calculation of the integral elastic cross sections for the present experimental conditions using the  $v_\Sigma$  and  $v_\Pi$  interactions obtained by the CEPA technique of Staemmler and Jaquet<sup>2</sup> is shown (dotted curves in Fig. 1) to reproduce the overall behavior but to underestimate the absolute magnitude. An extrapolation procedure on their computed potentials lead Staemmler and Jaquet,<sup>2</sup> to propose improved  $v_\Sigma$  and  $v_\Pi$  interactions which actually, as shown in Fig. 1 (dashed curves), yield integral cross sections much closer to our measurements. We take this as evidence that, although the computed values underestimate the cross sections, the extrapolation procedure indicates correctly in which direction a substantial improvement can be achieved.

Our procedure thus starts by assuming that the *anisotropy*<sup>7</sup>  $v_2 = \frac{2}{3}(v_\Sigma - v_\Pi)$  is correctly given by CEPA calculation. In fact, it can be verified, at least for the range of distances probed by our experiment (i.e., where van der Waals minima occur) that the extrapolation procedure proposed by Staemmler and Jaquet does not modify substantially the *difference*  $v_\Sigma - v_\Pi$ . Actually, some evidence is being accumulated for other systems in our laboratory<sup>8</sup> that, because of error cancellations, such a difference can be estimated even from not too sophisticated calculations better than the individual contributions. Having fixed the anisotropy  $v_2$ , we then adjusted the *spherical*<sup>7</sup> interaction  $v_0 = \frac{1}{3}(v_\Sigma + 2v_\Pi)$  by using a sufficiently flexible form to fit our data. The results of such a procedure are shown in Fig. 1 (continuous curve),